

Reliable Integration of Thermal Flow Sensors into Air Data Systems

1st Felipe Augusto Braga Viana
Programa de Pós-Graduação em Engenharia Elétrica
Universidade Federal de Minas Gerais
Belo Horizonte - MG, Brasil
felipeviana@ufmg.br

2nd Frank Sill Torres
Cyber-Physical Systems
German Research Center for Artificial Intelligence
Bremen, Germany

Abstract—Having in mind its impact on the security of air flight applications, there is a high demand for robust and reliable airspeed measurement systems. Thermal flow sensors are a recent proposal in order to circumvent the critical limitations of classic airspeed sensors and have the potential to considerably enhance the security of future aircrafts. This paper is a step towards the application of these sensors and explores how existing state-of-the-art reliability techniques can be applied for this new class of devices. Therefore, a detailed simulation model of a thermal flow sensors is setup in a redundant manner and widely applied voting mechanism are added to the system. Using extensive fault simulations, we explored the applicability of each mechanism for different fault classes and determined the most reliable solution. Results indicate that not the most complex but a more simpler method based on median estimation shows the highest robustness for this new kind of airspeed sensors.

Index Terms—Air Data System, Robustness, Reliability, Redundancy, Data Acquisition, Airspeed, Thermal flow sensors

I. INTRODUCTION

The movement of an aircraft is determined by the air characteristics at the current altitude as well by its geometric shape, its attitude and the relation between flight speed and airflow. Based on these informations it is possible to determine aerodynamic forces and momentums generated on the airplane, which are essential informations for pilots and automatic aircraft control systems in order to take correct decisions [1]. Having in mind the possible fatalities of an airplane crash, those measurements must be performed under the highest reliability constraints.

Air Data Systems (ADS) measure and process airflow information and provide its results to further instances, enabling the implementation of complex closed loop control techniques. In todays aircrafts, airspeed is measured using the so called pitot tube [2]. However, the main disadvantage of the pitot tube is that it can freeze during specific conditions such that all measurements performed by the sensor turn invalid. This was the reason for several flight accidents, e. g. the crash of the Air France flight 447 in 2009 with 228 fatalities [3].

Due to the possibility of failures on current airflow measurement systems and the catastrophic consequences of such a failure, there is a demand to study how to increase the

reliability of these measurements. One possibility is to use airspeed sensors with operating principles that differ from pitot tube. This, for example, the case for thermal flow sensors, which gained attention in recent years [4].

Although the working principles of thermal flow sensors is already known, there is still the need for further research before it can be used in commercial applications. This includes works on its physical implementation as well as on its integration in airplane systems. Based in these observations, the objective of this work is the exploration of how this type of sensors can be integrated in Air Data Systems (ADS) in robust and reliable manner.

The emphasis of this study is on how the impact of individual sensors faults on the results of ADS can be diminished. Therefore, we derived an appropriate model of the final sensors in order to assure that the final solution is robust against a wide range of possible faults. Further, we compared state-of-the-art redundancy techniques in terms of its applicability for thermal flow sensors.

The remainder of this work is as follows. Section II describes the state-of-the-art of aircraft speed measurement systems, thermal flow sensors and voting techniques. The following Section III presents the chosen methodology, while Section IV discusses its implementation. Section V shows and analyses the obtained results. Finally, Section VI concludes this work.

II. PRELIMINARIES

A. Air Data Systems

A typical commercial ADS integrates multiple sensors and processing units in order to provide critical air data parameters, including static and dynamic pressure, altitude, angle of attack and side slip [5]. Fig. 1 shows a six sensors ADS, each composed of a pitot tube and a processing unit. The pitot tube is the transducer that transforms physical quantity into an electric signal, that in its turn is digitalized and sent to be processed and consolidated on the Air Data Computer (ADC). Sensor redundancy is required in order to achieve the required level of safety on the aircraft operation. International norms

developed by special committees and specific documents issued by government agencies define the process of calculation and demonstration of required safety levels [6], [7].

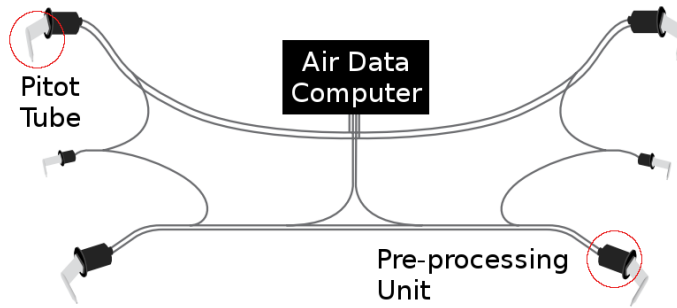


Figure 1. Representation of an ADS with six smart sensors and a processing unit [5].

B. Pitot Tube

The pitot tube is the transducer used in most ADS to convert physical quantities into electrical signals [2]. It consists of two concentric tubes held on a short distance from the fuselage of the aircraft to prevent interference from it in the airflow. The inner tube contains an opening aligned with the direction of movement and is responsible for measuring the total pressure caused by the movement of the body in the air. The outer tube contains openings perpendicular to the movement and is responsible for measuring the static pressure of the environment. At the base of the tubes, transducers convert the pressures into electrical signals that are then digitized. The difference between total pressure and static pressure is called dynamic pressure and is used to calculate the relative velocity between the air and the pitot tube. The results of this measurement is called airspeed [1].

Under specific weather and air flow conditions, a pitot tube can freeze. In this case, the sensor can not measure the external, total or static pressures, making its measurements unreliable. In cases like these the pilot must realize that the speed measurement is wrong and ignore it, navigating through other instruments and visual points. Doing this is not trivial, and faults of this kind have caused recent crashes, such as the aforementioned crash of the Air France flight [3]. Another restriction of the sensor is that it must be aligned with the movement flow, within a maximum allowable deviation, to correctly measure speed. The pitot tube also interferes with the aerodynamics of the airplane and therefore the quantity and location of the sensors must be carefully studied in order to guarantee redundancy and performance.

C. Thermal Flow Sensor

There is an extensive line of research on thermal flow sensors, as we can see in the bibliographic study of [4]. All sensors are based on the principle of measuring the velocity of a fluid through the thermal interaction between this fluid and the sensor. Despite the common principle, there are several

types of configuration, materials and applications for thermal flow sensors. Based on the study of [4], a sensor that was close to the imagined application for this work is described in [8] and [9]. This sensors was developed in order to operate in the air, has a large operation range, is capable of measuring speed and direction of flow, has improvements over a commercial thermal flow sensor and has a full functioning model. The thermal flow sensor is depicted in Fig. 2 and consists of four temperature sensors (thermopile) and four heaters (resistors) arranged at the edges of a square silicon chip. In addition, the component contains a diode in the center of the chip that measures the average temperature of the chip and the control logic required for sensor operation.

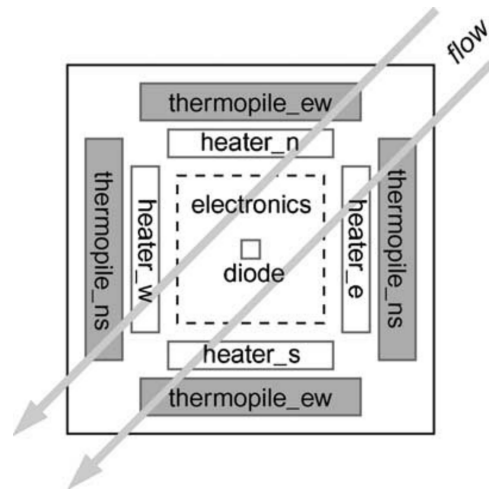


Figure 2. Components of a thermal flow sensor [9].

The asymmetrical cooling effect is considered in each thermopile in order to measure the speed and the direction of the air flow through the sensor. As can be seen in Fig. 2, given a horizontal right-to-left flow, the east-west thermopile will be cooled asymmetrically by losing more heat at the right side than at the left side. There are two "ew" sensors placed in parallel and connected in series in order to increase the sensitivity of the thermal asymmetry. The same effect happens when there is a vertical flow, in which the asymmetric cooling occurs in the north-south components (ns).

A Sigma Delta thermal modulation technique is used to keep the sensor operating at constant temperature. The thermal asymmetry detected by the thermopiles is in a closed loop feeding the choice of which heater should be driven in order to correct the measured difference. A comparator connected to the thermopile output creates a series of pulses that turn on or off the related heaters. For example, if the comparator detects the east side cooler than the west side then the east heater is turned on.

This operation technique eliminates the need for an ADC to obtain system measurement. The output of the speed sensor is the bit stream representing the power dissipated by each resistor. The information needed to calculate the speed is the

power difference between the opposing resistors. Thus, the difference between the power of the resistors "e" and "w" is called δP_{ew} and the difference between the resistors "n" and "s" is called δP_{ns} . The velocity of the flow is proportional to the sum of the squares of δP_{ew} and δP_{ns} and the direction of the flow is obtained by considering the values of δP as the orthogonal components of the velocity vector. The values obtained with this sensor have a maximum error of 4% for speed and 4° for the direction of flow [9].

The equations (1), (2) and (3) determine the flow speed and direction from δP_{ew} and δP_{ns} [8]. In these equations, ϕ is the flow calculated direction, U is the flow calculated speed; a_{ns} and a_{ew} are differences due to thermal asymmetries; S_{ns} and S_{ew} are proportional factors; ε_{ns} and ε_{ew} are phase differences from the reference on direction guidance; δP_{ns} and δP_{ew} are the differences of the heater powers.

$$\phi = \tan^{-1} \left(\frac{v_{ns} \cos(\varepsilon_{ew}) - v_{ew} \sin(\varepsilon_{ns})}{v_{ns} \sin(\varepsilon_{ew}) + v_{ew} \cos(\varepsilon_{ns})} \right) \quad (1)$$

$$U = \frac{v_{ns}^2 + v_{ew}^2 - 2v_{ns}v_{ew} \sin(\varepsilon_{ns} - \varepsilon_{ew})}{\cos^2(\varepsilon_{ns} - \varepsilon_{ew})} \quad (2)$$

$$v_{ns} = \frac{\delta P_{ns} - a_{ns}}{S_{ns}} \quad v_{ew} = \frac{\delta P_{ew} - a_{ew}}{S_{ew}} \quad (3)$$

As can be seen in [9], the thermal flow sensor is protected from direct contact with the airflow by being secured to a thin ceramic ceramic disk which separates it from the object of measurement. This configuration is an advantage in the aeronautical application because the sensor can be placed in the most suitable place of the fuselage of the aircraft without interfering in its aerodynamics.

D. Voting Techniques

Voting techniques are frequently applied for redundant signal consolidation [10]. There are several implementations that differ in its complexity and robustness against different types of faults.

A common solution is the estimation of the simple mean of the input signals of the voter. This is the simplest way to reduce the influence of a failed signal on the consolidated value of the measure, although it does not remove its influence. Another technique is to calculate the output as the median of the input signals. In the case of an odd number of signals this corresponds to choosing the middle signal to be equal to the output. In the case of an even number of signals, this corresponds to making the simple average of the two signals in the middle.

In addition to these two types, the authors of [10] propose the majority average voting, in which the difference between the input signals is compared to a predefined range Δ . When the differences are less than Δ the signals are considered

valid and the output is the average of all that have met the requirement. If the difference of one signal to the others is greater than the threshold, it is not considered in the calculation. If the distribution of the signal values is such that the difference between them is less than the threshold in more than one subset of signals, then that subset having the most signals is chosen for the calculation. For example, in case of four input signals, signals A, B and C may happen to fulfill the criterion of Δ and signals C and D as well. In this case, the subset ABC that contains most of the signals is chosen.

The authors of [11] introduce a variation of the majority average, where the threshold value is not used. In this technique, two signals that have the smallest difference between them are chosen among all the available ones and the output is the average of them.

A more complex voting algorithm is presented in [12]. This technique differs from the others because it is not a simple formula for calculating the output, but a series of fault-detection algorithms that work in parallel, constantly analyzing the input signals. If no fault has been detected and all input signals are considered valid, the output is the median of all input signals. If the algorithm detects a fault in one of the input signals then the incorrect signal is removed from the voting and the median is calculated with the remaining signals.

The techniques for detecting signal faults are described below:

- Compare: If the difference between an input signal and the voted value of the output in the previous cycle was greater than a predefined threshold, it is considered to have a *compare* fault.
- Range: If the value of an input signal is outside the predefined operating limits, it is considered to have an *out of range* fault.
- Oscillation: If only one of the signals is oscillating within a predefined frequency range and with an amplitude greater than a threshold, that signal is considered to have an *oscillating* fault.
- Split: If four signals are in a two pair configuration with close values within the pair but distant values between the pairs, using preestablished thresholds, they are considered having a *split* fault. In this case all signals are considered to be faulty.

Each fault detection algorithm contains filters to perform time dynamic analysis of the signals and criteria to consider a valid signal again after a fault is detected. In addition, the output is altered in a damped manner at each change in the number of signals considered to be valid.

III. METHODOLOGY

The objective of this work is the exploration of the applicability of well established voting methods for an Air Data System composed of thermal flow sensors. Therefore, a simulation model of the thermal flow sensor proposed in [8] was derived and modified for fault simulation. Next, the results

of selected state-of-the-art voting mechanism were compared [10]–[12].

Among the considered voters, the model of [12] requires four input values, while the others do not have a fixed number of inputs. Due to this configuration, the use of a redundancy system with four thermal flow sensors was chosen to properly compare all voters.

The test environment is depicted in Fig. 3. The main system inputs are the values of δP_{ns} and δP_{ew} (summarized as *power asymmetry*), from which the modeled sensors 1 to 4 calculate the airspeed values. The values of the first four sensors are distributed within a range of $\pm 4\%$, following from the experimental results obtained in [9]. A fifth *Reference sensor* is used in order to calculate the reference airspeed value. The input of this sensor has no deviation and its output is the ideal result of the airspeed measurement.

The faults in sensors 1 to 4 are modeled via modifications of the parameter a_{ns} (shown as *Faults* in Fig. 3), which represents the difference due to the thermal asymmetry of each thermocouple. The insertion of this fault in the model results in behaviors that are specific to the chosen sensor and allow the study of the ability of the voting techniques to deal with this type of faults [9].

The outputs of the sensors 1 to 4 are used as inputs to the voting algorithm to be tested, which then generates a consolidated airspeed value. This value is compared to the reference value of the reference sensor. The difference between the voted value and the reference value is a measure of the voter performance on removing fault interference from the consolidated velocity.

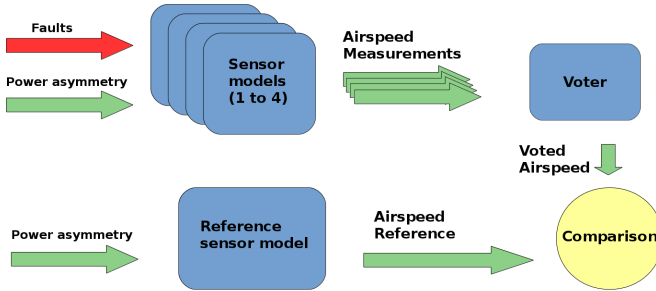


Figure 3. Simulated system components and data flow diagram.

Simulations are done by varying several input parameters, i. e. shape of the input signal; input value; frequency of the input signal; type of dependence between fault and input; error value associated with fault; location and number of faults.

IV. IMPLEMENTATION

We used a Matlab simulation environment in order to model the thermal flow sensor and to perform the analysis of voting techniques. The thermal flow sensor model was constructed based [8]. It is basically the implementation of the mathematical formula that represents the relationship between

the power differences δP_{ns} , δP_{ew} , the speed and direction characteristics of the airflow. The electronic circuit behind the sensor was not considered in the model. As we have already described, the fault considered in the sensor is represented via the parameter a_{ns} .

Models of all the described voters were implemented so that they could be used in the simulations. Due to the complexity of the voter proposed by [12], was done as follows: (1) construction of the model; (2) isolated test of each macro-component described with predefined inputs and outputs; (3) integrated test of the complete voter with predefined input signals in order to observe the operation of the system. These steps were important to ensure extensive model verification before its use on the target simulation. In addition, this voter has a number of parameters that modify its operation and should be chosen for each application. The implementation process also involved the choice of the most appropriate parameters for the application of the thermal flow sensor with its operating characteristics.

The integration of the blocks followed the data flow presented in the methodology section, with the addition of scripts to make the input choices, simulation and results analysis.

V. RESULTS

The simulations were performed according to what was proposed in the methodology section (III). The parameters were independently varied for each of the entries present in Table I and Table II, being that the faults were chosen according to the sensor model [9]. The frequencies were not independently varied for constant input and ramp due to the nature of these signals. In total 2880 different simulations were done.

Table I
INPUT PARAMETERS

| Type | Value | Frequency (Hz) |
|------------|-------|----------------|
| Constant | 1 | 0,25 |
| Ramp | 2 | 1,25 |
| Sinusoidal | 3 | 2,5 |
| Rotational | - | 10 |
| - | - | 25 |

The constant input type assumes one of the listed values and has no time variation. The ramp type is a signal that grows at a constant rate, ranging from 0 to twice the set value for input. The sinusoidal input has zero constant component and amplitude and frequency equal to the chosen values. The rotational input is more peculiar because it represents the situation in which a constant velocity flow equal to the chosen value changes the direction in which it passes through the sensor. This means that this input has different values for δP_{ns} and δP_{ew} , varying in time in sinusoidal and co-sinusoidal form. Since each direction is an orthogonal component of the velocity of the flow, the velocity amplitude is constant.

Faults are entered into the specified sensor by changing the value of the parameter a_{ns} . The constant type changes

Table II
FAULT PARAMETERS

| Type | Value | Location |
|--------------|-------|--------------|
| Constant | 0.5 | Sensor 1 |
| Ramp | 1 | Sensor 2 |
| Proportional | 2 | Sensor 1 e 2 |
| Derivative | 4 | Sensor 1 e 4 |
| - | 8 | - |

the parameter to the value chosen by the whole simulation. The ramp case is similar to the input, with the value going from 0 to 2 times the specified value. In the proportional case, the thermal unbalance parameter is equal to the sensor input multiplied by the chosen value of the fault. In the derivative case, the same multiplication, but considering the derivative of the input. Fig. 4 shows exemplary the output of a sensor for different fault types. The input is of rotational type with value 2 and frequency of 0.25Hz, the amplitude of the fault is 2.

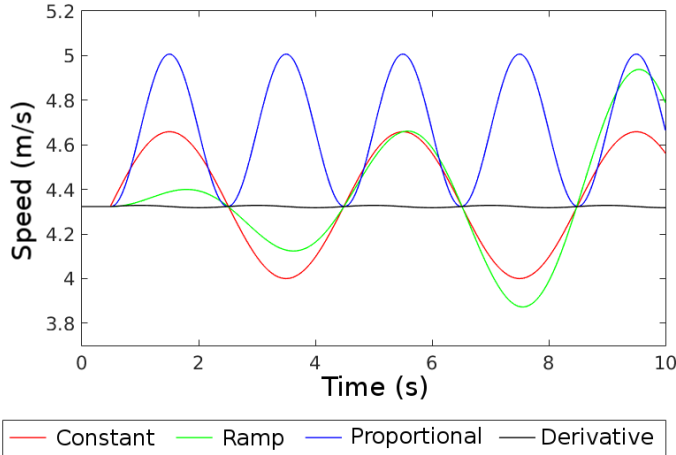


Figure 4. Output of the thermal flow sensor for different fault types while having rotational input at 0.25Hz.

It is possible to compare the voter's performance by observing the average and maximum error of each one. For our analysis, *voter 1* means the one proposed by [12]; *voter 2* is the simple median, *voter 3* refers to the simple mean; *voter 4* the majority average [10] and *voter 5* is the mean of the two nearest signals proposed by [11]. For the first analysis stage of the data, the results of the simulations were separated by the location of the faults and the frequency of the input chosen as 0.25Hz.

The average error of *voter 2* is significantly smaller than the other voters for faults only in sensor 1 or only in sensor 2, remaining less than 2% for these cases. In the case of double but opposite faults (sensors 1 and 4) *voter 2* also performs better, with an error around 0.1%. In the case of neighboring double faults (sensor 1 and 2) the average error of *voter 2* is very close to *voter 3* but both are still the best, falling

below the 4% threshold. These comparisons can be observed in Fig. 5.

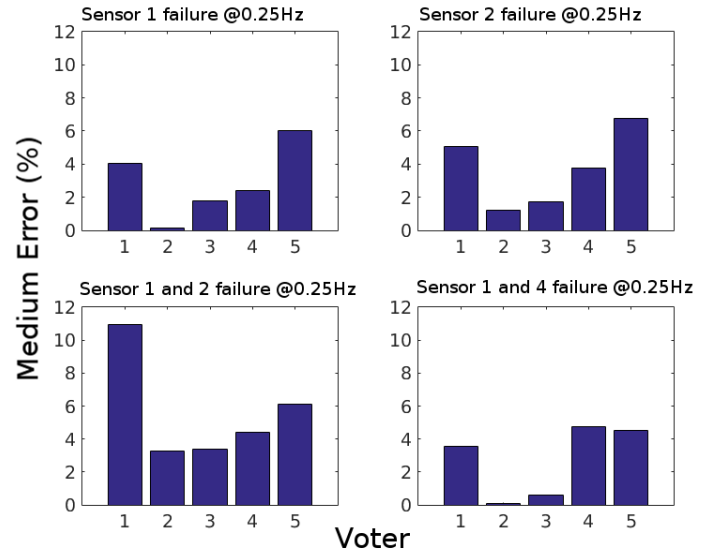


Figure 5. Medium error of the voters for different fault locations.

A similar analysis can be made for the maximum error. For single or double opposing faults *voter 2* is clearly better, reaching at most error of about 23%. For two neighboring faults, *voter 2* loses the highest-scoring position and reaches error of 218%. In this particular case, *voter 4* and *voter 5* have better performance, with maximum errors approaching 63%. Especially *voter 1* performs much worse than the others when we observe the maximum error, reaching 655% in the worst case. The graph in Fig. 6 summarizes this analysis. It is important to note that in this figure the graph scale of the faults in sensor 1 and 2 is different from the others to show the maximum value.

The analysis of the input frequency influence on the performance of the voters is done by observing how the mean error changes with increasing frequency for faults in sensor 1. This is depicted in Fig. 7. It can be observed that the average error of *voters 2-5* were not influenced by the frequency. *voter 1*, on the other hand, had a large increase in average error with increasing frequency, reaching the level of 15% at 25Hz. An analysis of the influence of the frequency on the maximum error shows a similar behavior, as shown in Fig. 8. Only *voter 1* is worse with increasing frequency, reaching an error of 200% at 25Hz.

Considering this analysis it is possible to conclude that *voter 2*, whose output is the median of the input signals, has the best performance if applied in an ADS composed by four redundant thermal flow sensors. This voter significantly reduces the influence of simple faults, regardless of location, and opposing double faults. In the case of neighboring double errors, *voter 2* maintains the lowest average error among the analyzed methods, but loses the lowest maximum error

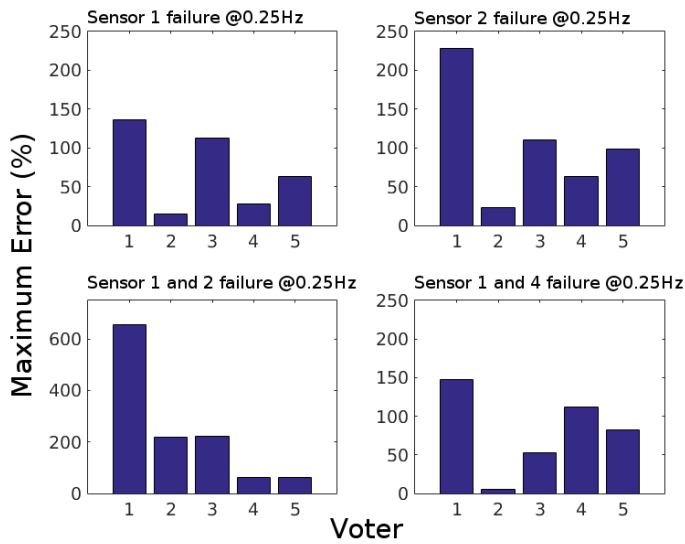


Figure 6. Maximum error of the voters for different fault locations.

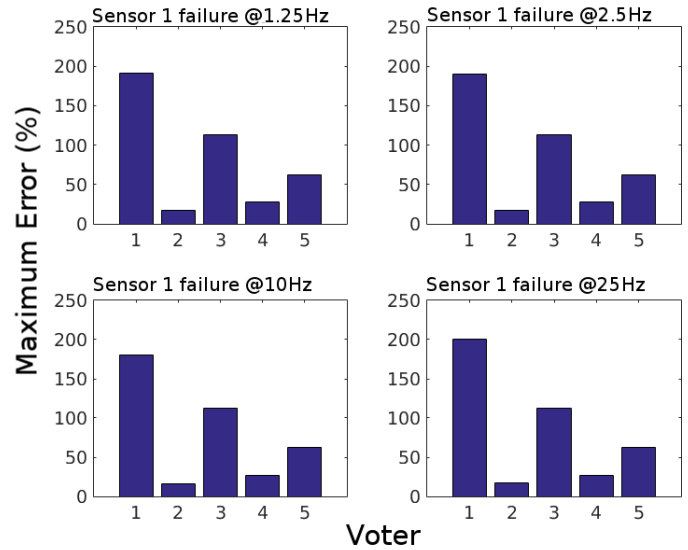


Figure 8. Maximum error of the voters for different frequencies.

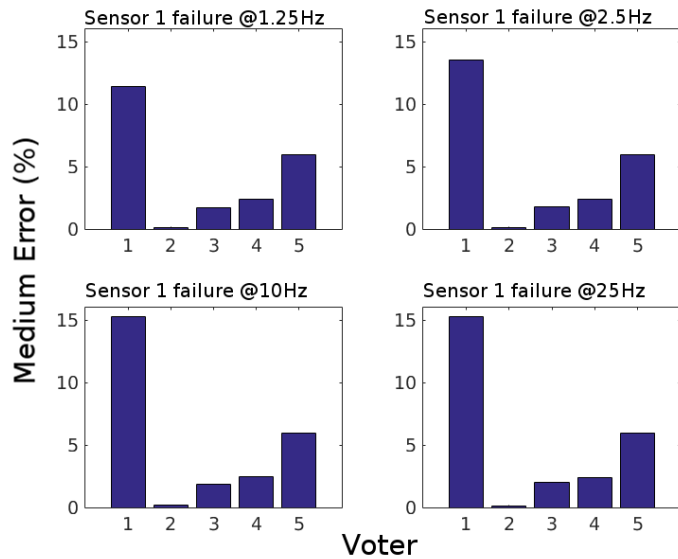


Figure 7. Medium error of the voters for different frequencies.

position to *voter 4* and *voter 5*, which use the mean of the nearest signals.

Voter 1 has an irregular performance and was the worst in several of the analyzed cases. He was expected to have one of the best performances due to some factors. Its most basic operating principle is the same as for *voter 2*, that is, if none of the parallel error detection techniques are triggered, the output is the median of the inputs. All of its other error-detection techniques work in parallel and have very specific goals, which should increase the scope of the voter. His performance was expected to be equal to *voter 2* in the worst case and better than it overall. This leads to the conclusion that the error detection techniques of *voter 1* are degrading its performance. Especially

when observing the good performance of the *voter 2* in simple faults for the most different types of errors and signal forms, the complex techniques present in *voter 1* are unnecessary in this case. The ideal would be to use such techniques only to remove signals from voting on complex faults.

By observing more closely the behavior of *voter 1*, it is noted that its performance is worse for oscillatory and rotational inputs, a fact that was already indicated by its response to higher frequencies (Fig. 7). This behavior occurs because of the voter removing and reinserting the signal that it considers to be wrong. By doing this the fade-out of *voter 1* kicks in, causing a significant delay in the voter's output. This analysis reinforces our conclusion that the error-detection techniques of *voter 1* worsen its performance for simple errors, which can be observed in Fig. 9 which compares *voter 1* and *voter 2*. This graph nicely shows the recurrent error peaks, each one happening when *voter 1* output is faded at a slower rate than required by the oscillating signals. The output of *voter 2*, on the other hand, eliminates the inserted error.

The configuration of faults in sensors 1 and 2 at the same time is the most complicated to be analyzed and corrected by the voters. In practice, if a system with four sensors has a double fault and the values of the faulty sensors are close, it is impossible to know which pair of signals is closest to the true value. This is the simulated case that caused the worst results in the voters, and in which *voter 1* was the worst of all (Fig. 5 and Fig. 6), so this case deserves to be observed more carefully.

Analyzing the behavior of *voter 1*, one can see that the error data does not reveal the whole story of its operation. Its fault-detection algorithm relies on a "split" detection, as described in section II. This algorithm works as expected in the simulated case. It can be seen in Fig. 10 that *voter 1* detects

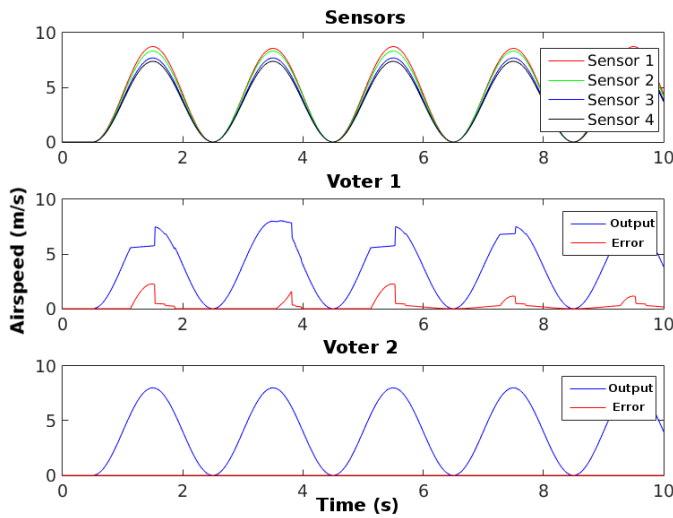


Figure 9. Output and error of voter 1 and voter 2 with oscillatory input @0.25Hz

the condition "split", and in doing so, freezes the output signal at the last value considered as valid. As the inputs continue to rise, the computed error of the voter becomes larger. On this condition the voter 1 also signalizes that its voted output is not reliable by setting all signals to false. This behavior diminishes the impact of an erroneous value as the systems is informed about this error.

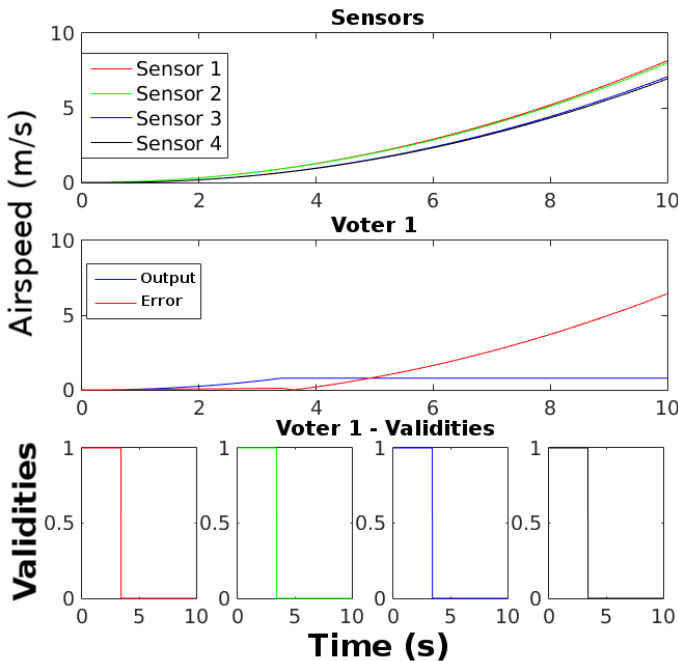


Figure 10. Voting output and validity for constant faults on sensors 1 and 2 and ramp input.

Considering the behavior of the voter 1 for the split case, we conclude that it would be the most appropriate for the case

of neighboring double faults in the thermal flow sensors.

VI. CONCLUSION

Measurement of airspeed is of great importance for the safety of aeronautical applications. Thermal flow sensors offer to circumvent the critical limitations of classic airspeed sensors and are intended to be the basis of future Air Data Systems. In view of this development, this work explores how state-of-art reliability methods can be applied to these new sensors. The results indicates that an Air Data System using four redundant thermal flow sensors and a single median-based voter offers the best performance. It is also possible to conclude that in the event of a sensor fault, the application of a more sophisticated voter results in a measurement error greater than for simpler solutions. However, in the case of similar double faults, a system using a voter able to detect split condition has an advantage in being able to catch and report this fault. It can be concluded that the results of this work are a step towards the design of Air Data Systems using thermal flow sensors on high reliability aeronautical systems.

ACKNOWLEDGMENTS

The authors are grateful to CAPES, CNPq and FAPEMIG for the financial support of this work.

REFERENCES

- [1] Nelson, Robert C.: *Flight Stability and Automatic Control*. McGraw-Hill Book Company, 1st edition, 1989.
- [2] Andersson, Bengt J.: *On measurement of velocity by pitot tube*. Ark. Mat., 3(5):391–394, January 1958.
- [3] BEA: *Final Report On the accident on 1st June 2009 to the Airbus A330-203*. Bureau d'Enquetes et d'Analyses, 2012.
- [4] Haasl, Sjoerd and Göran Stemme: *Comprehensive Microsystems Chapter 2.07: Flow Sensors*. Elsevier Science, 2007.
- [5] UTC: *SmartProbe® Air Data Systems*. UTC Aerospace Systems, 2015.
- [6] SAE: *Guidelines and Methods for Conducting the Safety Assessment Process on Civil Airborne Systems and Equipment*. SAE International, 1996.
- [7] SAE: *Guidelines for Development of Civil Aircraft and Systems*. SAE International, 2010.
- [8] Makinwa, Kofi A. A. and Johan H. Huijsing: *A wind-sensor interface using thermal sigma delta modulation techniques*. Sensors and Actuators A 92 (2001) 280-285, 2000.
- [9] Makinwa, Kofi A. A. and Johan H. Huijsing: *A smart wind sensor using thermal sigma-delta modulation techniques*. Sensors and Actuators A 97-98 (2002) 15-20, 2001.
- [10] S. Askari, M. Nourani and A. Namazi: *Fault-tolerant a/d converter using analogue voting*. IET Circuits, Devices & Systems, 2011.
- [11] Alves, Emerson M. A. and Frank S. Torres: *Aumento de confiabilidade de sistemas embutidos usando redundância e algoritmos de decisões baseados em reconhecimento de padrões*. XXI Congresso Brasileiro de Automática - CBA2016, 2016.
- [12] Oliveira, Livia Camargos Rodrigues de and Roberto Kawakami Harrop Galvao: *A four-signal voting algorithm for aircraft redundant sensors*. 21st Brazilian Congress of Mechanical Engineering - COBEM 2011, 2011.